

Article

# Correction of Thermal Errors in Machine Tools by a Hybrid Model Approach

Christian Friedrich \*, Alexander Geist, Muhammad Faisal Yaqoob, Arvid Hellmich and Steffen Ihlenfeldt

Fraunhofer Institute for Machine Tools and Forming Technology, Reichenhainer Str. 88, 09126 Chemnitz, Germany; muhammad.faisal.yaqoob@iwu.fraunhofer.de (M.F.Y.)

\* Correspondence: christian.friedrich@iwu.fraunhofer.de; Tel.: +49-351-4772-2625

**Abstract:** Thermally induced position errors are one of the main error sources on the workpiece caused by the behavior of the machine tool. In today's industrial environment, the correction of thermal errors is usually based on simple regression approaches, where the characteristic diagrams for correction are generated experimentally. The performance of these approaches is only valid for the corresponding load regimes, which often results in insufficient correction quality in practical applications. Consequently, there is only a limited benefit or even a deterioration in machine behavior if the correction characteristic is based on an inapplicable load case compared to the initial experiment. Simulation-generated characteristic diagrams using finite element models solve this disadvantage, but do not answer the question about the choice of the right characteristic matching the current load situation, and, in addition, calculate very slowly. Structural model-based correction using reduced models, on the other hand, calculates quickly, but requires a high modeling effort for accurate correction. The approach, presented in this contribution, combines simulation-generated characteristic diagrams and a structural model-based decision algorithm for a new hybrid model in order to select the appropriate characteristic diagram for the present load situation in the control system. This paper presents the simulative characteristic diagram generation by a finite element model validated by experiments in a climate chamber and a validated structural model including the concept for the decision algorithm.

**Keywords:** machine tools; thermal error correction



**Citation:** Friedrich, C.; Geist, A.; Yaqoob, M.F.; Hellmich, A.; Ihlenfeldt, S. Correction of Thermal Errors in Machine Tools by a Hybrid Model Approach. *Appl. Sci.* **2024**, *14*, 671. <https://doi.org/10.3390/app14020671>

Academic Editor: Qiang Cheng

Received: 8 December 2023

Revised: 4 January 2024

Accepted: 6 January 2024

Published: 12 January 2024



**Copyright:** © 2024 by the authors. Licensee MDPI, Basel, Switzerland. This article is an open access article distributed under the terms and conditions of the Creative Commons Attribution (CC BY) license (<https://creativecommons.org/licenses/by/4.0/>).

## 1. Introduction and State of the Art

In machine tools, thermo-elastic structural deformations cause up to 75% of the machining inaccuracies measurable on the workpiece [1,2]. Hereby, thermal errors in machine tools are considered to be much more relevant than geometric, static, and dynamic errors [3,4]. Nevertheless, the correction of thermally induced errors in the development and operation of machine tools is currently regarded as insufficiently solved and a recognized problem in industry [4]. Established procedures are specific to machine, load case, and environmental boundary conditions [5]. This is a particular issue for Small- and Medium-sized Enterprises (SMEs), as they usually have small batch sizes, a wide range of parts, and heterogeneous machinery as well as usually no air conditioning for machine tools available [6]. Whereas large companies, as series producers, regard thermal-related faults in operation as dominant and worthy of correction, small- and medium-sized companies regard the problem of thermal behavior as too complex to tackle. Time- and energy-inefficient warming-up phases or complicated temperature control strategies produce significant costs, along with potential rejects. During the summer months, temperature fluctuations of 5 to 15 Kelvin during the day occur, which increases the need for a suitable correction procedure [7–9]. Consequently, the performance of the machine tools falls short of what is theoretically possible [10].

The available approaches are divided into compensation and correction methods, where the first aim to minimize or prevent the occurrence of thermally induced deformations by influencing heat inputs and heat flows, and the latter aim to correct the thermally induced displacements at the tool center point (TCP) by adapting the movement specifications [11,12]. Examples for compensation methods are thermo-symmetric structure design, temperature control of drives, bearings and guides, frame components, as well as temperature control of the cooling lubricant, partly by evaluation of the ambient temperature based on a reference sensor as well as air conditioning of the environment and air cooling [13–16]. However, compensation methods are often expensive and do not include internal heat sources. In addition to other approaches, for example, using learning algorithms [17–23], the main approaches for correction methods are characteristic diagram-based correction and structure model-based correction, as outlined next.

### *1.1. Characteristic Diagram-Based Correction*

Characteristic diagrams represent a set of input variables continuously mapped onto defined output variables. Between support points, data can be generated by multilinear interpolation, polynomials, B-splines, or other functions, depending on the type of the diagram [24]. Characteristic diagrams are largely independent of the structure they describe, making this approach flexible and locally applicable at the component level. In the state of the art, characteristics are currently mostly determined from experimental results. Alternatively, characteristic diagrams can also be obtained very efficiently by simulation based on finite element (FE) models using temperature and displacement fields [25]. These models are characterized by a very good representation of the temperature fields [26]. Because the physical machine tool is not required to generate the characteristic map, it is possible to create a wide variety of load case configurations by means of calculations based on the FE model that has been created and calibrated once. This modularization reduces the computational effort and enables the assignment of locally relevant input variables to each component input variable [27]. Current research focuses on the development of efficient grid structures of high-dimensional characteristics and FEM with multigrid solvers [28–30]. FEM-based sensitivity analysis is used to determine the optimal positions for temperature sensors as the basis of simulation-based characteristics, and smoothed grid regression is used in research work as an extended calculation methodology for characteristic diagrams [31]. It has been shown that a 40–80% reduction in the mean thermally induced error can be achieved through the application of simulation-based characteristics [32–34] and even more, when the characteristics can be updated with information regarding the current load case [35–37].

### *1.2. Structure Model-Based Correction*

In contrast to the characteristic diagram approach, the structural model-based correction method includes the structural variability and calculates the temperature and displacement field based on the moving structure and current pose. In consequence, heat inputs can be applied to moving components, such as feed axes, in the specific locations where they occur [38,39]. The structural model is not necessarily based on FEM approaches but also uses physical-based models on a system or digital block simulation, such as Matlab/Simulink® or ESI ITI SimulationX®. It includes partial models for power loss, thermal coupling coefficients, and thermo-elastic displacement and approaches for calculating the axis correction values. A modular strategy for correcting structure models in the context of machine tools has been developed through fundamental research and is undergoing validation on numerous machine components and structures [36,40–43]. The modules can be divided into three areas: data acquisition, modeling, and correction, whereby each area is calculated in its own time domain (control real time and thermal real time) that can be calculated decoupled from each other (control internal and control external). It can be shown for a machine component that the thermally induced position error could be reduced by 80–87% for a machine component “bar axis” [41]. In ref. [44], the

error components of the rotational axes were corrected with the help of a physical model; a reduction in the error between 35% and 38% was achieved.

Regarding characteristic diagrams, for each load case, as it depends on the workpiece and each machine tool, a suitable characteristic diagram must be determined experimentally, which is highly inefficient [4,32]. The high costs are a major obstacle to the introduction of correction methods. Simulation-generated characteristic diagrams, on the other hand, allow a certain load case variability right up to the option to generate several characteristics in parallel for multiple load cases and are more cost-efficient. However, the simulations are very time-consuming (48 h for one load case for the simulated DMU80) and the choice of the correct characteristic as a basis for correction as well as methods for changing the characteristics on the running machine are still open research questions. Finally, structure models can include the current load situation and simulate quickly but require a huge modeling effort to achieve sufficient accuracy for thermal error correction.

Consequently, the development of a cheap and smart hybrid correction methodology that takes the changing load cases (e.g., different workpieces), the specifics of the machine, and the changing environmental conditions into account, allows for a reduction in costs, scrap rate, and inefficient warm-up phases, and, at the same time, an increase in workpiece quality.

This paper presents a new hybrid model approach that combines the advantages of simulation-generated characteristic diagrams and structural models with a decision algorithm to achieve a cheap and smart correction technology for machine tools.

## 2. Approach

The objective is to develop a hybrid correction method that combines a list of simulation-generated characteristic diagrams with a structural model-based observer as the decision maker in order to activate the appropriate characteristic regarding the present load situation in the machine tool control system that is used for thermal error correction.

To do so, a thermo-elastic FE model was generated for the test machine tool DMG Mori DMU 80 evolution and validated by extensive experimental studies including various thermal load cases. Next, the FE model was qualified to generate simulative characteristic diagrams resulting in a “Characteristic Generator”, Figure 1 left, that also can be validated by the experimental studies. With this, a variety of characteristics for different load cases can be generated and stored in a database, where they are available for selection by the “Numeric Control” (NC), Figure 1 bottom. However, there is currently no method available to find and activate the most appropriate characteristics depending on the current load case of the machine tool. In the presented approach, a fast-calculating structural-based model order reduction (MOR [45]) model was build up and validated that is able to simulate current load situations from linked machine data and was used to evaluate the actual correction quality, Figure 1 right. The outstanding feature of the hybrid model is the addition of the observer, Figure 1 center, which continuously ensures with the help of the fast-calculating structural model that a valid characteristic diagram is used for correction in the control system. If the current correction is not sufficient, a suitable characteristic can be selected from the mentioned database, and, if there is none, the missing characteristic can be generated by interpolating existing characteristics or by new FE simulation with the stored load case description. In addition to the two model calculations, the approach includes, therefore, the observer to evaluate to current correction quality, the interfaces to the models and to the process data to automate the calculations, the database of previously calculated maps, and the interface to the numeric control to exchange the current correction diagram during production.

This paper presents in the following sections the experimental setup as the basis for FE model validation and experimental characteristic diagram generation (Section 3), the FE model and simulative characteristic diagram generation (Section 4), and the design and validation of the structural model (Section 5). The developed methodology was applied and illustrated exemplarily for the machine tool DMU 80 evolution.

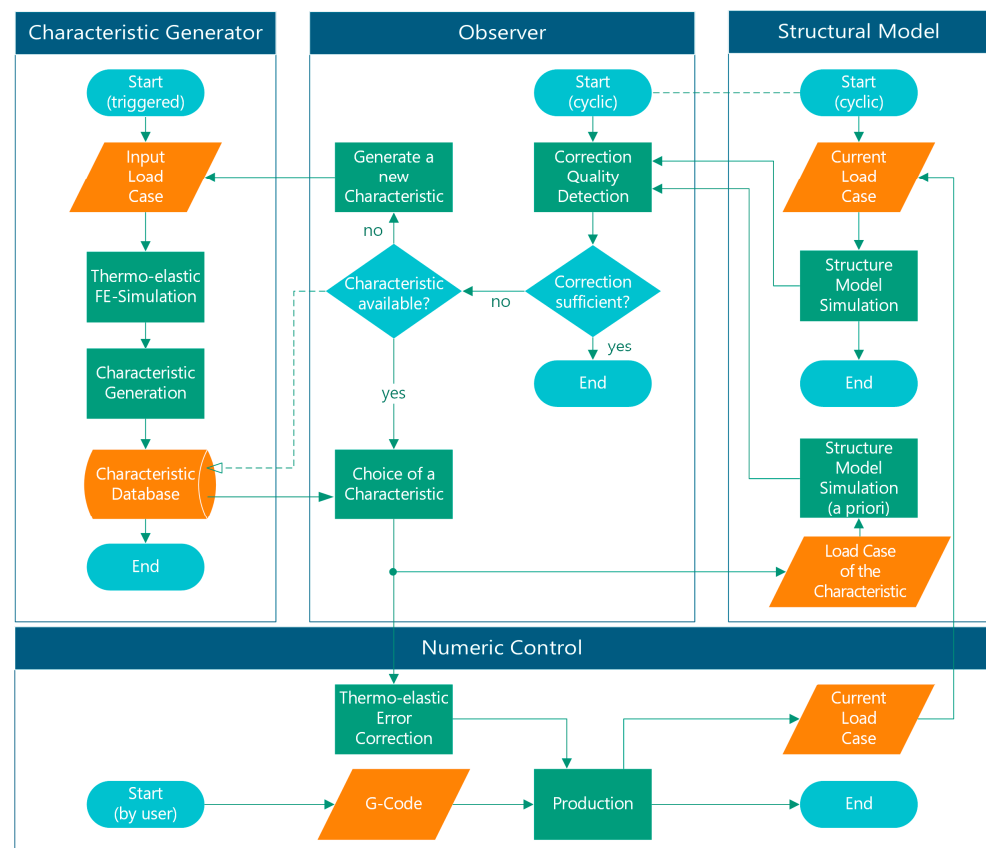


Figure 1. Architecture of the hybrid model approach.

### 3. Experimental Characteristic Generation

At first, a reference characteristic of the DMU80 machine tool was created by extensive thermal experiment studies that were, in addition, the basis for the validation of the created simulation models. The experiments were carried out on the demonstrator machine during operation in different load situations, where, at the same time, the physical variables of temperatures, displacements, motor currents, and axis speeds were recorded. To do so, a structured experimental plan was drawn up in order to provide meaningful load cases for the validation of the simulation calculations. This plan outlines the number, duration, and type of experiments, as well as an estimated workload for the measurements. Based on this, the measurement set-up with the corresponding sensors was practically built and the measurement data acquisition system was set up. When carrying out the experiments, care was taken to eliminate as many disturbance variables as possible and to ensure that the target variable could be sufficiently resolved so that a clear distinction could be made from measurement noise at all times. The measurements were carried out on the DMU 80 evo in a stationary climate chamber (Figure 2), which allows the ambient and ground temperatures to be controlled. In addition, the climate chamber offers a wide range of options for the climate control, which was used for the experiments:

- Setting of a fixed ambient temperature in the range of 10–40 °C;
- Regulation of the air humidity to a stable value of 50%;
- Control of the floor temperature in the range of 15–30 °C;
- Variation of the ambient temperature in a day–night cycle (sine wave).

A cooling lubricant module with a capacity of up to 900 L was available for the test machine, which was equipped with a cooling unit with a capacity of up to 6 kW. The temperature of the cooling lubricant was recorded at all times.

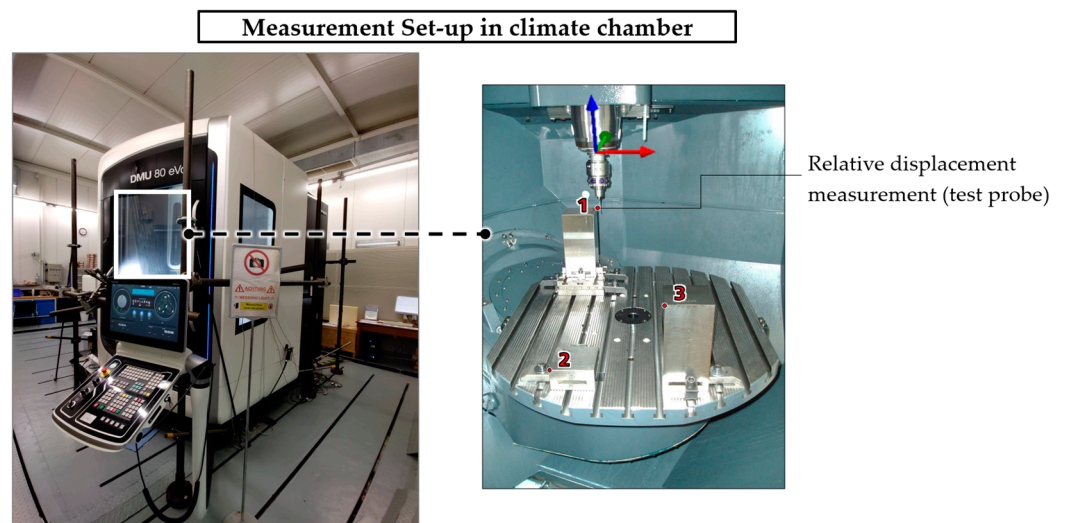


**Figure 2.** Demonstrator machine tool in the climate chamber (left) and displacement-measuring probes (right).

Further operational parameters of the machine are the type of coolant supply (external coolant supply through side nozzles, coolant supply through tool, and bed flushing) and the internal and external heat sources. The internal heat sources arise from the power loss of moving machine components (bearings and motors) due to friction and winding losses in electric motors. These are mainly caused by the rotary motion of the table, the motor spindle, and the rotation of the swivel axis. External heat sources include chips during the machining process and heating pads, which are used in experiments to introduce heat in a specified manner. For experiments without machining (air cuts), the external heat sources are omitted.

In the experimental design, the heat sources within the machine and the environmental influences due to cooling lubricant and global ambient temperature were considered and investigated in a decoupled manner, Table 1.

**Table 1.** Excerpt of the design of experiments and sequence of measurements.

	Tool Axis	Linear Travel Axes			Rotatory Table Axes	
	Spindle	X	Y	Z	B	C
	0	0	0	0	0	0
Load in %	50	25	25	25	25	25
	100	75	75	75	75	75

The basic experimental plan was divided into three main blocks. In the first main block, the influence of the cooling lubricant on an unmoved machine was investigated at a previously defined and stable ambient temperature. The parameters temperature, volume flow, and type of supply were varied. In the second main block, the temperature of the cooling lubricant was controlled as stably as possible, whereby the parameters of the ambient temperature and machine load (internal heat sources), expressed as the percentage of the maximum travel speed of the machine, were considered separately, Table 1. In the third and last main block, practical load cases were examined and considered in order to verify the correction approaches developed in the project. Hereby, the change in ambient temperature, room-temperature-controlled cooling lubricant temperature, but also machining processes were included. These investigations can also be carried out outside a climate chamber and are intended to prove the newly developed simulation approaches for practical use. Finally, a characteristic diagram was created based on the experimental and simulative results and used for classic thermal error correction so far.

Figure 3 shows an example measurement for an ambient temperature change in a 24 h cycle. Three of the twenty integrated temperature sensors (T2–T4) are shown as a time–temperature curve. Also, air and ground temperatures are presented, where the air temperatures were recorded at two different heights (50 cm and 200 cm). On the right side of the diagram, the relative displacement between tool center point and the workpiece side is shown for an example point. Further details regarding the experimental studies in the climate chamber and the validation of the models are presented in the literature [46].

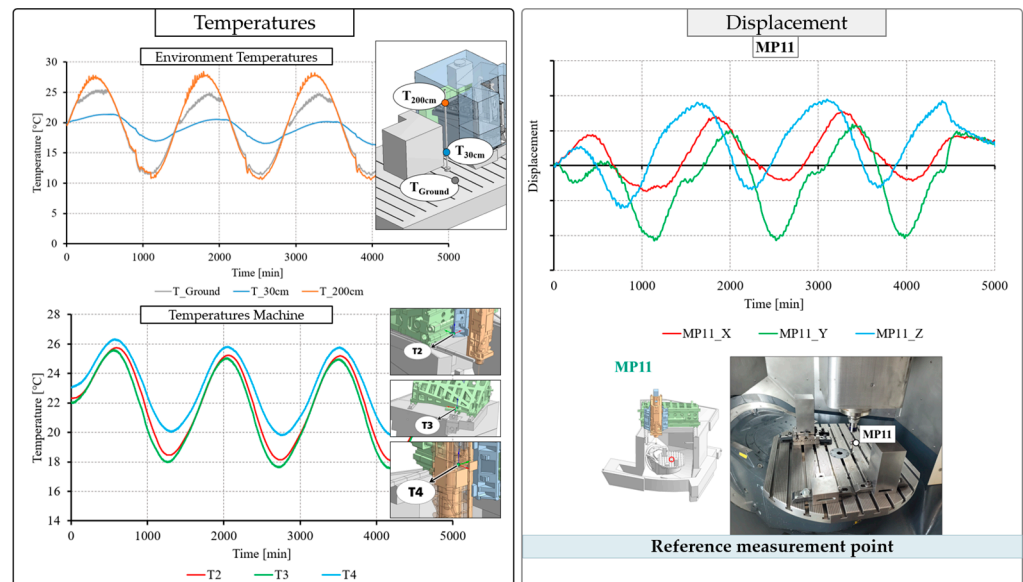


**Figure 3.** Example of a measurement with a change in ambient temperature.

#### 4. FE Model and Simulative Characteristic Generation

Following the approach, the next step was to create characteristics by simulation instead of experiments with the help of a thermo-elastic finite element model. This model was created based on a CAD geometry model of the entire machine that needed to be reduced in complexity: At first, detailed design features (e.g., small holes and bores) were removed in the design environment and complex bodies were simplified. These included screw connections, guide rails, bearings, and motors. This was necessary as otherwise there could have been issues with the meshing or an unnecessarily high number of FE elements would have been created. Non-relevant assemblies such as the machine housing and switch cabinet were removed. Next, the data were exported in a neutral CAD exchange format.

The subsequent import took place in the simulation environment ANSYS Workbench, where the meshing and calculation were performed in ANSYS Mechanical. With the help of the software, it was possible to carry out a static mechanical analysis based on a thermal analysis that was calculated in advance. The calculated temperature field served as a thermal load for the calculation of the deformation field when compared to a reference state. The relative or absolute displacements of the tool center point (TCP) in all three spatial coordinates (X, Y, and Z) could be determined from the deformation simulation. Figure 4 shows the entire workflow of the simulation process. The individual model phases are explained in more detail below.

The CAD model was divided into further sub-assemblies, which were later reassembled after the meshing level in the simulation level in order to be able to map the different axis positions (see Figure 4). In the Ansys Workbench, the individual subsystems were assembled as building blocks to form an overall system, while each unit could be processed independently at the submodel level. This allowed a good overview and structure of the overall project, because the overall model of a machine tool is very complex. The most important properties, such as material data, were included in a separate database.

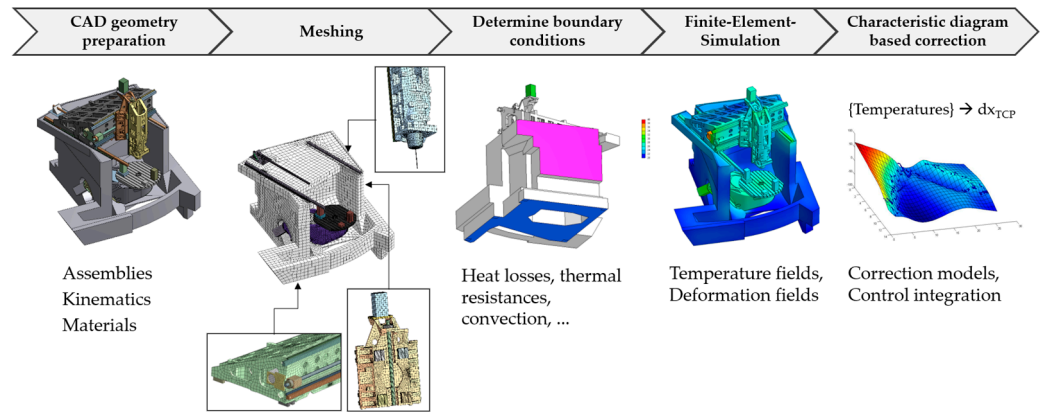


**Figure 4.** Workflow for the creation of a finite element machine model.

The following Figure 5 shows the simplified machine model and the FE mesh on which it was based. The individual solid bodies were decomposed into simple finite volume elements (e.g., tetrahedron and hexahedron). The primary emphasis of the modeling was on achieving high-quality elements while minimizing the total number of volume elements to reduce both computational and storage requirements.

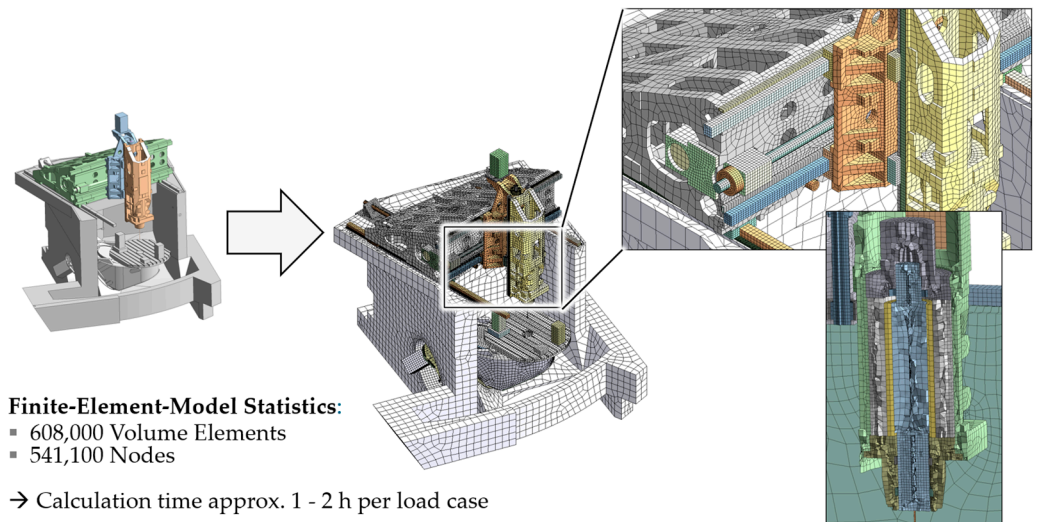


**Figure 5.** Three-dimensional geometry of the machine and volume mesh.

The model boundary conditions included all possible types of heat flows and convective boundary conditions needed to solve the heat conduction equation in the FE solver. The model’s boundary conditions were modified as required to achieve the closest approximation to the physical model possible, Figure 6. This was achieved by considering the internal heat sources in the machine, such as heat-loss of motors and motor spindle, frictional heat in bearings, and guides.

In order to be able to simulate and represent a machine behavior (axis movements) that is as universal as possible, individual areas of the active surfaces were segmented. This was achieved, for example, for the running surface of the guideway and the spindle shaft of the ball screw, Figure 7. Asymmetric load cases can also be applied, by introducing an average heat flow locally to the running area of the guideways, as presented in Figure 7. Flow effects, such as cooling lubricant or heat exchange with the environment, are described by a heat transfer coefficient, whereby the individual assembly surfaces are clustered.

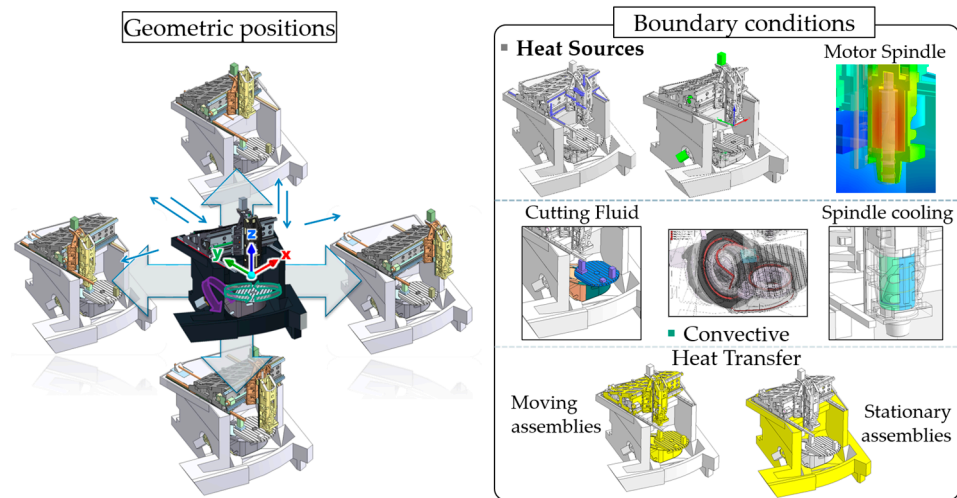


Figure 6. Overview of possible thermal boundary conditions.

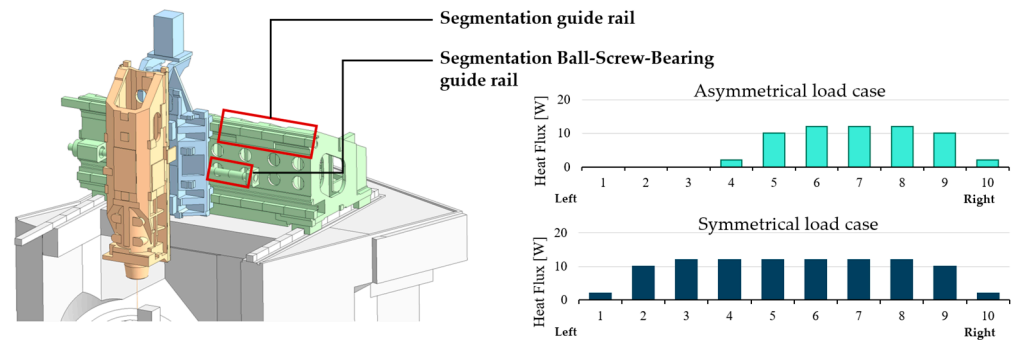


Figure 7. Area segmentation and allocation of local heat fluxes.

Finally, with the help of the FE solver, the transient temperature field was calculated for a defined load case and, in the final step, the static deformation of the entire machine compared to a reference state was calculated for each time step. Post-processing was also performed at this level to display the temperature and displacement fields of the simulation, Figure 8.

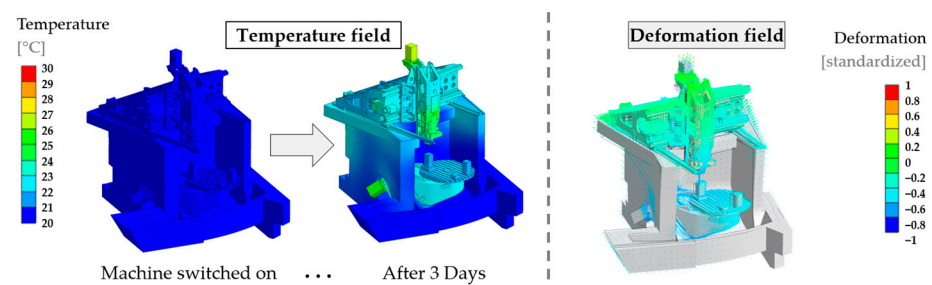


Figure 8. Visualized simulation results of the FE calculation (example).

A script interface was used to read the physical data at discrete monitor points, especially sensor points of the temperature measurement as well as relative displacement measurement between tool center point and the workpiece. Read from the solution file and stored in text files, these data can then be used for offline training of a characteristic diagram correction.

Once programmed, the characteristic diagrams provide the correction offset values for the TCP in the X, Y, and Z directions at any time. The rotation axes of the table (B and C) were corrected by an angle. The main input variables are temperature sensors and the

current actual positions of the axes. However, other input variables, such as motor currents or accelerations, can also be used if required. A computer integrated within the machinery calculates real-time correction values from characteristic diagrams and transfers them to the Numeric Control, as shown in Figure 9.

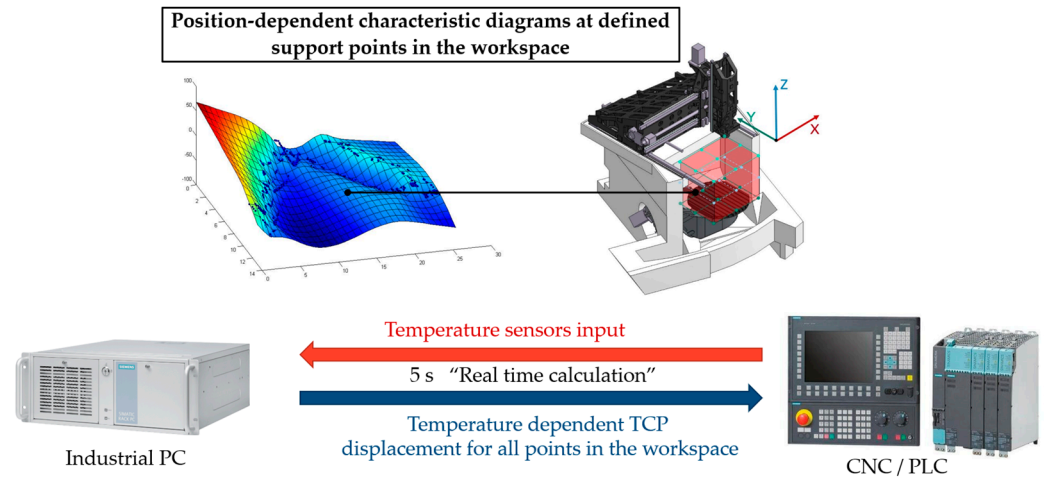


Figure 9. Integration of the map correction into the NC control system.

With the help of the NC control, the calculated offset values were added to the running CNC program and thus the error was corrected. Because a single characteristic diagram usually does not achieve the required complexity, several characteristic diagrams are usually connected at discrete support points (e.g., at defined zones in the working area). This is due to the fact that large characteristic diagrams require a lot of memory and computing power for their creation, because the computational effort grows exponentially with each additional input variable. In practice, it is therefore beneficial to use several less complex characteristic diagrams in a network.

For validation of the simulation-generated characteristics, several experiments with and without activated characteristic diagram correction were performed. In the experiment, heat input was achieved by axis movements, which led to thermally induced displacements at the TCP, Figure 10. It is a combination of the load cases which were already simulated. The results from the simulation were used to train the characteristic diagram correction. It shows that almost all reference measuring points can achieve very good correction values of up to 90% and that the characteristic diagram correction therefore works very well for the trained load cases. However, characteristic maps have their limitations at unknown load cases, as stated in the introduction. Therefore, a fast-calculating structural model was used to evaluate the validity of the currently activated characteristic diagram, as outlined next.

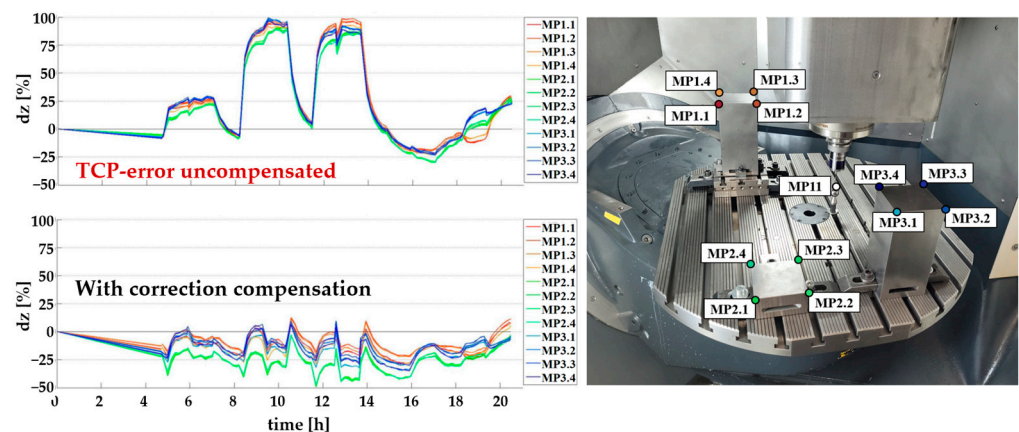


Figure 10. Validation of the compensation on selected load cases.

### 5. Structural Model

The structural model is an essential component of the hybrid correction approach. It entails the responsibility to provide on-demand evaluations of the current load case to the decision algorithm for validity and accuracy checks. The structural model was built in MATLAB from a reduced CAD model and allows structure changes during simulation. Figure 11 provides an overview on the implementation process of the structural model, divided into five steps.

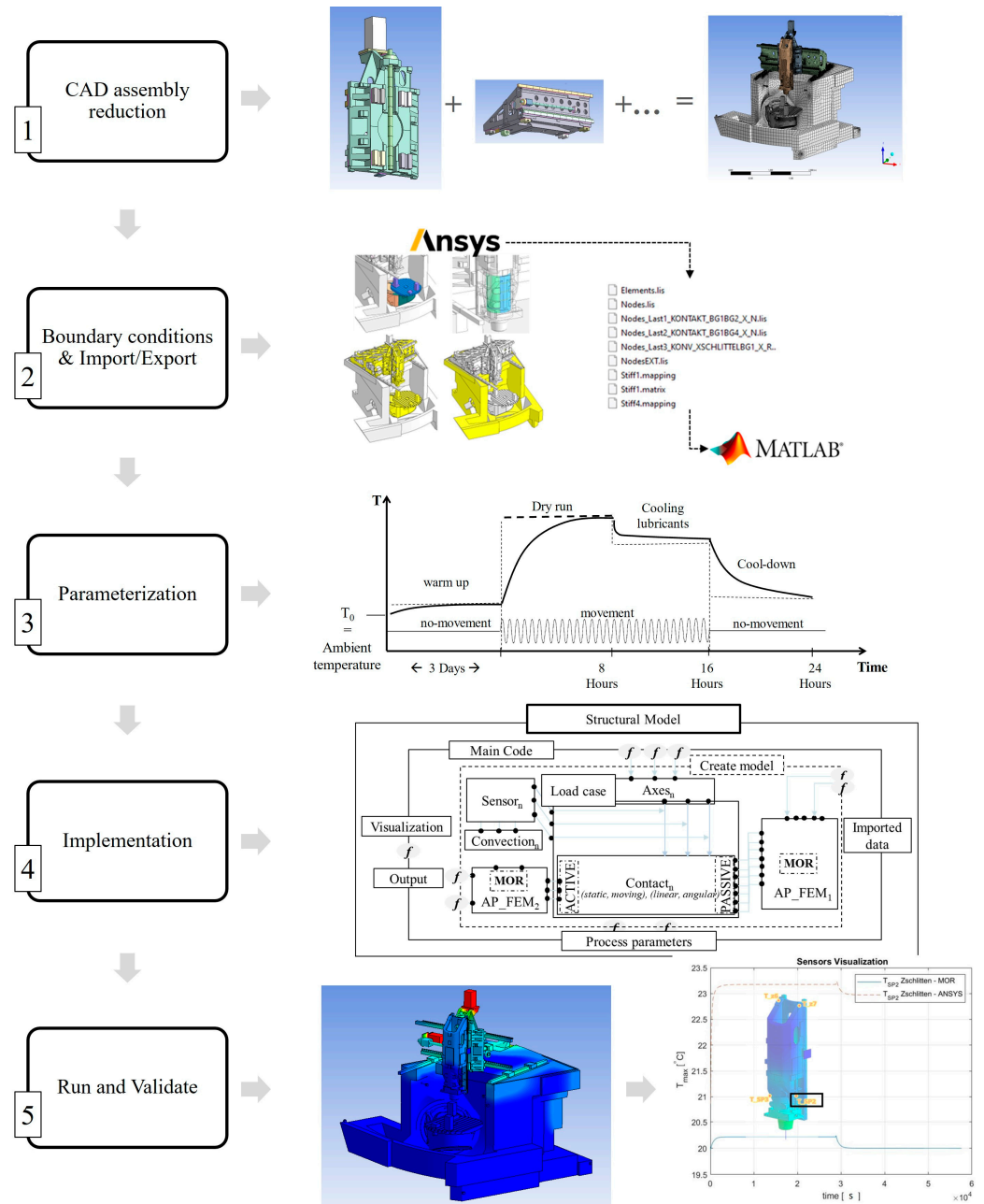


Figure 11. Structural model implementation.

The first step was to create a 3D CAD model of the machine and reduce the overall machine based on relative movements and static assembly parts. The demonstrator machine DMU 80 was reduced to six parts as illustrated in Figure 12. Once the machine was divided based on relative movements, it was necessary that each assembly part (AP) was meshed in ANSYS individually based on linear tetrahedral elements and shared topology. For external heat flow to another AP, conformity is not recommended for sliding interactions

due to unsteady heat flow (e.g., all six parts as in Figure 12 should have non-conformity with respect to each other; therefore, specific moving contact scripts were produced).

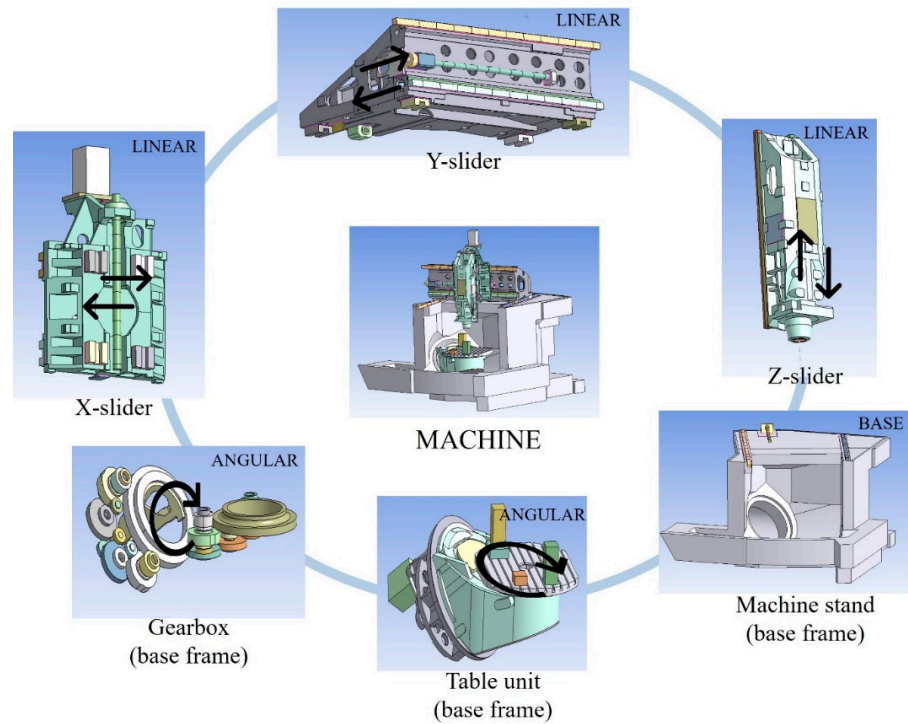


Figure 12. Machine assembly reduction based on relative movements.

The second step involved preparing the model for export by performing individual exports for each AP. Ansys Parametric Design Language (APDL) scripts were used to export the geometrical and material parameters required for the processing of structural model blocks in MATLAB. Once all generated files were gathered, the process flow of the machine was implemented along with the control’s data, experiment data, and process parameters onto the physical blocks in a structural model framework accordingly, which was basically parameterization and implementation (steps three and four). The structural model was generally a block diagram simulation (BDS) made of various blocks as defined in [47]. Each of these blocks defines a specific task to do, and steps three and four (Figure 11) mainly happen in this framework. A rough illustration of the used framework of the structural model to calculate thermal load for two assembly parts (AP1 and AP2) moving against each other with input load case data is shown in Figure 13.

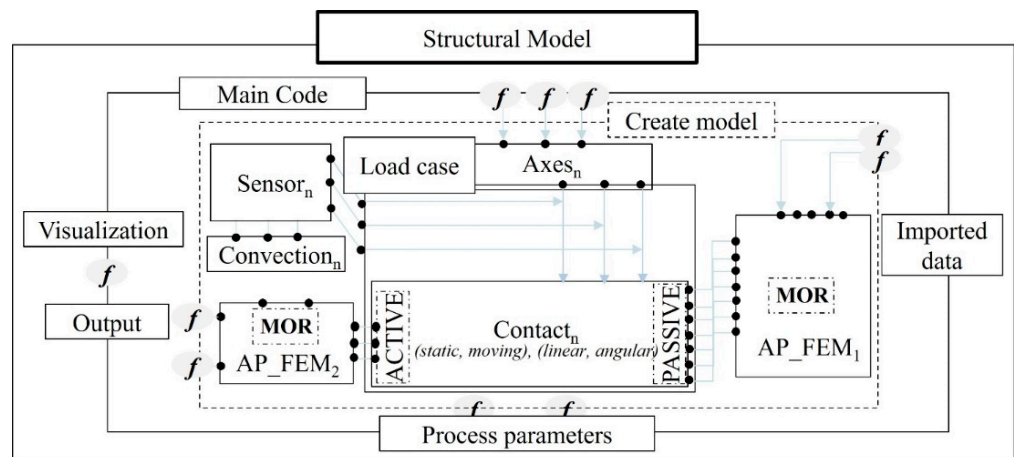


Figure 13. Framework of MOR-based structural model (code-based blocks in MATLAB).

Table 2 highlights an outline of the key features exhibited by significant components of the structural model.

**Table 2.** Block characteristics of structural model.

Block	Description
Main Code	Here, the interconnections of each block are defined and with the help of additional function scripts ( $f$ ), the overall process parameters are implemented and performed, such as time domains (solver time step, data sampling rate, and correction rate), machine model calculation, pre-processing of imported data, post-processing of the output, and visualization.
Create Model	A complete machine is assembled including the imported data of each AP, contacts, sensors, axes, convection blocks, and FEM-to-MOR pre-processing. Once the configuration of sub-blocks is finalized, creation of the model is a one-time process and the created model can later be directly loaded into the main code saving compilation time for different load cases.
Sensor	Heat flow/generation scripts are generated separately for each surface to impose thermal values found by experiments.
Convection	Scripts are generated separately for each surface to impose convection values found by experiments on specific renamed imported surfaces.
Axes	Spatial parameters are defined and prepared to gather data from the load cases incoming from machine controller. These load cases together with axes block are then communicated to moving contact blocks for thermal load calculation.
Contact	Contacts could either be linear or angular and moving or static. Depending on the case, the respective contact block is generated. In the presented case, contact scripts mainly act as a medium to incorporate load case by machine controls and generate a position-dependent temperature profile. These scripts work simultaneously, i.e., active AP contact + passive AP contact, with other blocks.
FEM block	Finite Element Modeling (FEM) numerical procedure is introduced and integrated with CreateModel and Main Code.
MOR block	Krylov-based Model Order Reduction (MOR) method is introduced, which is used to downsize the DOF of whole system and retransform into temperature points for output block.

Step five finally involves transitioning the structural model into Run Mode after ensuring the readiness of the parameters, blocks, functions, and data. Once the model is error-free, executable, and validated with the FE model on static boundary conditions, the machine controls data are incorporated.

The load (control) data consist of current, position, speed ( $I$ ,  $x$ , and  $v$ ), and ambient temperature. Data tracing from the machine is performed at a sampling interval of 4 ms ( $t_{data}$ ). Conventional methods for implementing relative movements between assemblies to generate position-dependent load profiles often involve detecting contact positions at each position change, which can be computationally intensive and slow for online correction. However, the presented approach eliminates the need for physical movement between assemblies altogether, providing a more efficient and faster alternative. The idea is to continuously collect data in a solver block at the given data sampling rate and average the collected data signals to calculate position-dependent loads through the pre-programmed moving contact scripts as concluded in [41]. Figure 14 shows a graphical representation of the mentioned approach.

The moving contact scripts incorporate heat equations to calculate thermal loads accordingly with changing thermal conductions and are case-dependent based on active–passive AP movement. In FE simulation, segments are created, and a similar approach is used in structural modeling. Segmentation allows for the simulation of asymmetric load cases (e.g., one-sided heat input on the right side). For example, if a moving part slides over a static part (denoted by vertical arrows), one of them is divided into several segments and after every 10 s of solver time step, 2500 signals of data (i.e., based on a 4 ms data sampling rate  $\rightarrow 10/0.004 = 2500$ ) are averaged over the divided segments to generate a position-dependent load profile. Preliminary results indicate feasible approximation of thermal behavior when tested with the control's data, i.e., load cases. The structural model is subjected to a series of tests to investigate the simulation time. Figure 15 elaborates on the simulation time comparison and a temperature profile visualization of the structural model.

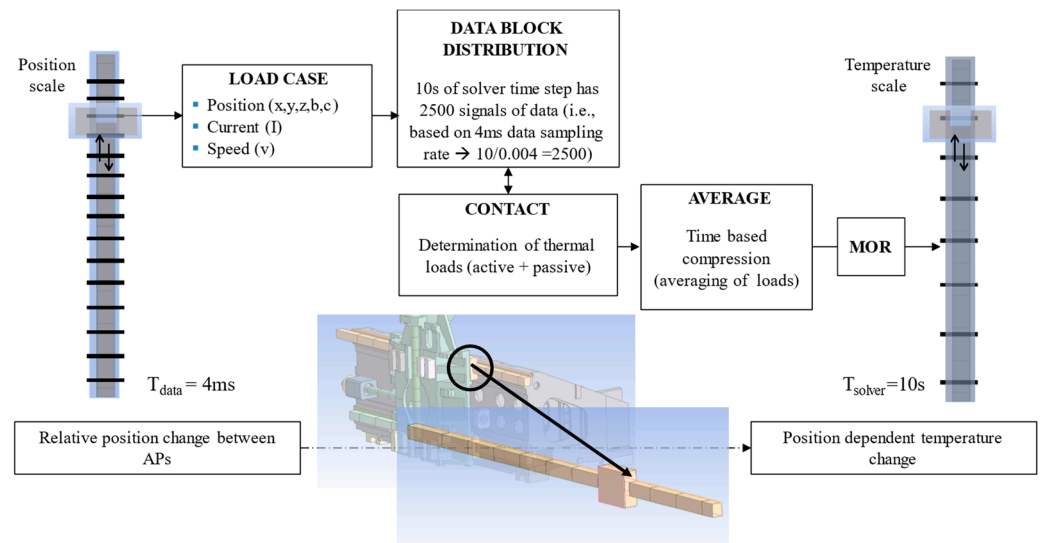


Figure 14. Contact implementation between moving APs for position-dependent loads.

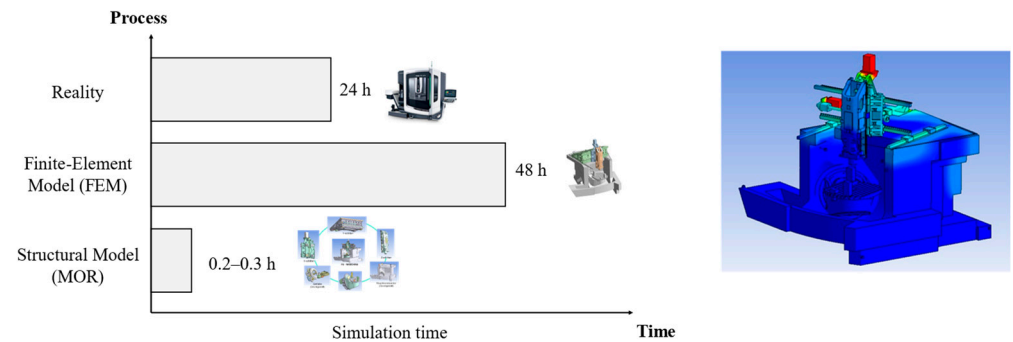


Figure 15. Comparison of simulation time among real machine process, FEM, and structural model (left) and graphical representation of thermal behavior of complete machine (right).

An example load case was simulated in both the FE model and the structural model. A comparison between the two models revealed an error ranging from 10% to 15% (subject to change with further development) in the structural model when compared to the FE model, while exhibiting similar temperature behavior. It was further observed that 24 h of reality was simulated in 48 h through a conventional FEM procedure (ANSYS), while a structural model based on MOR (MATLAB) took less than 30 min. The structural model’s significant reduction in simulation time enhances its suitability for real-time decision making. This includes ensuring the accuracy of the current load case in the machine and determining the need for a new characteristic diagram.

### 6. Conclusions

Along the path to a hybrid thermo-elastic correction model that includes simulation-generated characteristic diagrams and a structural model, the FE model as well as the structural model are presented. Further, the models were validated by experimental studies and characteristic diagrams were created in experimental and simulative ways. It was shown that both the FE model and the structural model provided good calculation results compared to the measured data. With the help of the developed characteristic diagram-based correction, the error could be reduced by 40–60% on average. With these components now ready, the next steps are the development and implementation of the observer and decision algorithms and the implementation within the numeric control system.

**Author Contributions:** Conceptualization, C.F., A.G. and M.F.Y.; methodology, C.F., A.G. and M.F.Y.; software, M.F.Y.; validation, A.G. and M.F.Y.; formal analysis, A.H.; investigation, A.G.; resources, S.I.; data curation, A.G.; writing—original draft preparation, C.F., A.G. and M.F.Y.; writing—review and editing, C.F.; visualization, A.G. and M.F.Y.; supervision, S.I.; project administration, C.F.; funding acquisition, A.H. All authors have read and agreed to the published version of the manuscript.

**Funding:** The project was funded by the German Federal Ministry for Economic Affairs and Climate Action with the program Industrial Collective Research and the project HybridThermo (22221 BR).

**Data Availability Statement:** Data are available on request due to restrictions.

**Acknowledgments:** The authors want to thank the editors and reviewers for their helpful comments and constructive suggestions with regard to the revision of this paper.

**Conflicts of Interest:** The authors declare no conflicts of interest. The funders had no role in the design of the study; in the collection, analyses, or interpretation of data; in the writing of the manuscript; or in the decision to publish the results.

## References

- Putz, M.; Richter, C.; Regel, J.; Bräunig, M. Industrial relevance and causes of thermal issues in machine tools. In Proceedings of the 1st Conference on Thermal Issues in Machine Tools, Dresden, Germany, 21–23 March 2018.
- Gebhardt, M.; Ess, M.; Weikert, S.; Knapp, W.; Wegener, K. Phenomenological compensation of thermally caused position and orientation errors of rotary axes. *J. Manuf. Process.* **2013**, *15*, 452–459. [CrossRef]
- Mares, M.; Horejs, O.; Fiala, S.; Lee, C.; Jeong, S.M.; Kim, K.H. Strategy of Milling Center Thermal Error Compensation Using A Transfer Function Model and Its Validation Outside of Calibration Range. *MM Sci. J.* **2019**, *2019*, 3156–3163. [CrossRef]
- Mayr, J.; Jedrzejewski, J.; Uhlmann, E.; Alkan Donmez, M.; Knapp, W.; Härtig, F.; Wendt, K.; Moriwaki, T.; Shore, P.; Schmitt, R.; et al. Thermal issues in machine tools. *CIRP Ann.* **2012**, *61*, 771–791. [CrossRef]
- Mayr, J.; Pavlicek, F.; Züst, S.; Blaser, P.; Hernandez-Becerro, P.; Weikert, S.; Wegener, K. Keynote. Thermal error research, an overview. In Proceedings of the Lamdamap 12th International Conference & Exhibition, Wotton under Edgem, UK, 15–16 March 2017.
- Dispan, J. *Entwicklungstrends im Werkzeugmaschinenbau 2017: Kurzstudie zu Branchentrends auf Basis einer Literaturrecherche*; Working Paper Forschungsförderung No. 029; 2017. Available online: <https://www.econstor.eu/handle/10419/215961> (accessed on 4 January 2024).
- Zhang, C.; Gao, F.; Yan, L. Thermal error characteristic analysis and modeling for machine tools due to time-varying environmental temperature. *Precis. Eng.* **2017**, *47*, 231–238. [CrossRef]
- Shen, H.; Fu, J.; He, Y.; Yao, X. On-line Asynchronous Compensation Methods for static/quasi-static error implemented on CNC machine tools. *Int. J. Mach. Tools Manuf.* **2012**, *60*, 14–26. [CrossRef]
- Mayr, J.; Ess, M.; Pavliček, F.; Weikert, S.; Spescha, D.; Knapp, W. Simulation and measurement of environmental influences on machines in frequency domain. *CIRP Ann.* **2015**, *64*, 479–482. [CrossRef]
- Wegener, K.; Weikert, S.; Mayr, J. Age of Compensation—Challenge and Chance for Machine Tool Industry. *Int. J. Autom. Technol.* **2016**, *10*, 609–623. [CrossRef]
- Großmann, K. *Thermo-Energetic Design of Machine Tools: A Systemic Approach to Solve the Conflict Between Power Efficiency, Accuracy and Productivity Demonstrated at the Example of Machining Production*; Springer International Publishing AG: Cham, Switzerland, 2015; ISBN 978-3-319-12625-8.
- White, A.J.; Postlethwaite, S.R.; Ford, D.G. A General Purpose Thermal Error Compensation System For CNC Machine Tools. *WIT Trans. Eng. Sci.* **2001**, *34*, 3–13. [CrossRef]
- Polyakov, A.N.; Parfenov, I.V. Thermal error compensation in CNC machine tools using measurement technologies. *J. Phys. Conf. Ser.* **2019**, *1333*, 62021. [CrossRef]
- Tseng, P.-C. A real-time thermal inaccuracy compensation method on a machining centre. *Int. J. Adv. Manuf. Technol.* **1997**, *13*, 182–190. [CrossRef]
- Liu, K.; Sun, M.; Wu, Y.; Zhu, T. Thermal Error Modeling Method for a CNC Machine Tool Feed Drive System. *Math. Probl. Eng.* **2015**, *2015*, 436717. [CrossRef]
- Naumann, C.; Fickert, A.; Penter, L.; Gißke, C.; Wenkler, E.; Glänzel, J.; Klimant, P.; Dix, M. Evaluation of Thermal Error Compensation Strategies Regarding Their Influence on Accuracy and Energy Efficiency of Machine Tools. In *Manufacturing Driving Circular Economy*; Kohl, H., Seliger, G., Dietrich, F., Eds.; Springer International Publishing: Cham, Switzerland, 2023; pp. 157–165, ISBN 978-3-031-28838-8.
- Abdulshahed, A.M.; Longstaff, A.P.; Fletcher, S.; Potdar, A. Thermal error modelling of a gantry-type 5-axis machine tool using a Grey Neural Network Model. *J. Manuf. Syst.* **2016**, *41*, 130–142. [CrossRef]
- Li, Y.; Yu, M.; Bai, Y.; Hou, Z.; Wu, W. A Review of Thermal Error Modeling Methods for Machine Tools. *Appl. Sci.* **2021**, *11*, 5216. [CrossRef]
- Blaser, P.; Pavliček, F.; Mori, K.; Mayr, J.; Weikert, S.; Wegener, K. Adaptive learning control for thermal error compensation of 5-axis machine tools. *J. Manuf. Syst.* **2017**, *44*, 302–309. [CrossRef]

20. Ma, C.; Gui, H.; Liu, J. Self learning-empowered thermal error control method of precision machine tools based on digital twin. *J. Intell. Manuf.* **2023**, *34*, 695–717. [[CrossRef](#)]
21. Zhu, M.; Meng, Z. Full compensation method of thermal error of NC machine tool based on sequence depth learning. *Int. J. Manuf. Technol. Manag.* **2023**, *37*, 138–150. [[CrossRef](#)]
22. Stoop, F.; Mayr, J.; Sulz, C.; Kaftan, P.; Bleicher, F.; Yamazaki, K.; Wegener, K. Cloud-based thermal error compensation with a federated learning approach. *Precis. Eng.* **2023**, *79*, 135–145. [[CrossRef](#)]
23. Zimmermann, N.; Büchi, T.; Mayr, J.; Wegener, K. Self-optimizing thermal error compensation models with adaptive inputs using Group-LASSO for ARX-models. *J. Manuf. Syst.* **2022**, *64*, 615–625. [[CrossRef](#)]
24. Priber, U. Smoothed Grid Regression. In *Proceedings Workshop Fuzzy Systems, Dortmund*; Mikut, R., Reischl, M., Eds.; Forschungszentrum Karlsruhe: Karlsruhe, Germany, 2003.
25. Weng, L.; Gao, W.; Zhang, D.; Huang, T.; Duan, G.; Liu, T.; Zheng, Y.; Shi, K. Analytical modelling of transient thermal characteristics of precision machine tools and real-time active thermal control method. *Int. J. Mach. Tools Manuf.* **2023**, *186*, 104003. [[CrossRef](#)]
26. Ess, M. Simulation and Compensation of Thermal Errors of Machine Tools. Ph.D. Thesis, ETH Zürich, Zürich, Switzerland, 2012.
27. Glänzel, J.; Kumar, T.S.; Naumann, C.; Putz, M. Parameterization of Environmental Influences by Automated Characteristic Diagrams for The Decoupled Fluid and Structural-mechanical Simulations. *J. Mach. Eng.* **2019**, *19*, 98–113. [[CrossRef](#)]
28. Naumann, C.; Riedel, I.; Ihlenfeldt, S.; Priber, U. Characteristic Diagram Based Correction Algorithms for the Thermo-elastic Deformation of Machine Tools. *Procedia CIRP* **2016**, *41*, 801–805. [[CrossRef](#)]
29. Putz, M.; Ihlenfeldt, S.; Naumann, C.; Glänzel, J. Optimized grid structures for the characteristic diagram based estimation of thermo-elastic tool center point displacements in machine tools. *J. Mach. Eng.* **2017**, *17*, 36–50.
30. Zwingenberger, C. Beitrag zur Verbesserung der Simulationsgenauigkeit bei der Bestimmung des Thermischen Verhaltens von Werkzeugmaschinen. Ph.D. Thesis, TU Chemnitz, Chemnitz, Germany, 2014.
31. Naumann, C.; Priber, U. Modellierung des Thermo-Elastischen Verhaltens von Werkzeugmaschinen Mittels Hochdimensionaler Kennfelder. In *Proceedings of the Workshop Computational Intelligence, Dortmund, Germany, 27–28 November 2014*; pp. 365–383.
32. Putz, M.; Ihlenfeldt, S.; Kauschinger, B.; Naumann, C.; Thiem, X.; Riedel, M. Implementation and demonstration of characteristic diagram as well as structure model based correction of thermo-elastic tool center point displacements. *J. Mach. Eng.* **2016**, *16*, 3.
33. Ihlenfeldt, S.; Naumann, C.; Putz, M. On The Selection and Assessment Of Input Variables For The Characteristic Diagram Based Correction Of Thermo-elastic Deformations In Machine Tools. *J. Mach. Eng.* **2018**, *18*, 25–38. [[CrossRef](#)]
34. Delbressine, F.; Florussen, G.; Schijvenaars, L.A.; Schellekens, P. Modelling thermomechanical behaviour of multi-axis machine tools. *Precis. Eng.* **2006**, *30*, 47–53. [[CrossRef](#)]
35. Naumann, C.; Glänzel, J.; Dix, M.; Ihlenfeldt, S.; Klimant, P. Optimization of Characteristic Diagram Based Thermal Error Compensation via Load Case Dependent Model Updates. *J. Mach. Eng.* **2022**, *22*, 43–56. [[CrossRef](#)]
36. Wenkler, E.; Hellmich, A.; Schroeder, S.; Ihlenfeldt, S. Part Program Dependent Loss Forecast For Estimating The Thermal Impact On Machine Tools. *MM Sci. J.* **2021**, *2021*, 4519–4525. [[CrossRef](#)]
37. Brecher, C.; Fey, M.; Wennemer, M. Correction Model of Load-Dependent Structural Deformations Based on Transfer Functions. In *Thermo-Energetic Design of Machine Tools*; Großmann, K., Ed.; Springer International Publishing: Cham, Switzerland, 2015; pp. 175–183, ISBN 978-3-319-12624-1.
38. Thiem, X.; Kauschinger, B.; Mühl, A.; Großmann, K. Challenges in the Development of a Generalized Approach for the Structure Model Based Correction. *Appl. Mech. Mater.* **2015**, *794*, 387–394. [[CrossRef](#)]
39. Thiem, X.; Großmann, K.; Mühl, A. Modular Control Integrated Correction of Thermoelastic Errors of Machine Tools Based on the Thermoelastic Functional Chain. *Adv. Mater. Res.* **2014**, *1018*, 411–418. [[CrossRef](#)]
40. Maier, T. Modellierungssystematik zur Aufgabenbasierten Beschreibung des Thermoelastischen Verhaltens von Werkzeugmaschinen. Ph.D. Thesis, TU München, München, Germany, 2016.
41. Thiem, X.; Kauschinger, B.; Ihlenfeldt, S. Online correction of thermal errors based on a structure model. *Int. J. Mechatron. Manuf. Syst.* **2019**, *12*, 49. [[CrossRef](#)]
42. Denkena, B.; Scharschmidt, K.-H. Kompensation thermischer Verlagerungen\*. *wt Werkstattstechnik online* **2007**, *97*, 913–917. [[CrossRef](#)]
43. Galant, A.; Beitelschmidt, M.; Großmann, K. Fast High-Resolution FE-based Simulation of Thermo-Elastic Behaviour of Machine Tool Structures. *Procedia CIRP* **2016**, *46*, 627–630. [[CrossRef](#)]
44. Gebhardt, M. *Thermal Behaviour and Compensation of Rotary Axes in 5-axis Machine Tools*; ETH Zürich: Zürich, Switzerland, 2014.
45. Großmann, K.; Galant, A.; Mühl, A. Effiziente Simulation durch Modellordnungsreduktion. *Z. Für Wirtsch. Fabr.* **2012**, *107*, 457–461. [[CrossRef](#)]
46. GEIST, A.; Naumann, C.; Glänzel, J.; Putz, M. Methods For Determining Thermal Errors In Machine Tools By Thermo-elastic Simulation In Connection With Thermal Measurement In A Climate Chamber. *MM Sci. J.* **2023**, *2023*. [[CrossRef](#)]
47. Beitelschmidt, M.; Galant, A.; Großmann, K.; Kauschinger, B. Innovative Simulation Technology for Real-Time Calculation of the Thermo-Elastic Behaviour of Machine Tools in Motion. *Appl. Mech. Mater.* **2015**, *794*, 363–370. [[CrossRef](#)]

**Disclaimer/Publisher’s Note:** The statements, opinions and data contained in all publications are solely those of the individual author(s) and contributor(s) and not of MDPI and/or the editor(s). MDPI and/or the editor(s) disclaim responsibility for any injury to people or property resulting from any ideas, methods, instructions or products referred to in the content.